Electronic structure, magnetic properties, Mössbauer isomer shifts, and hyperfine fields of disordered Fe-rich Fe-Al alloys

Hélio Chacham and E. Galvão da Silva
Departamento de Física, Instituto de Ciências Exatas (ICEx), Universidade Federal de Minas Gerais, 30161 Belo Horizonte, Minas Gerais, Brazil

Diana Guenzburger and D. E. Ellis
Department of Physics and Astronomy, Northwestern University, Evanston, Illinois 60201
(Received 30 July 1986)

The embedded-cluster model within the framework of the discrete variational method is used to carry out self-consistent-field electronic structure calculations for the isomer shifts, the hyperfine magnetic fields, and magnetic moments on several distinct iron sites in a disordered Fe-rich Fe-Al alloy. We analyze the dependence of those quantities on the number of nearest and next-nearest Al neighbors, on the symmetry of the local environments, and on lattice-parameter variation. Our results for the variations of the hyperfine field due to the presence of aluminum neighbors are in good agreement with experiment. The results for magnetic moments indicate that the antiferromagnetic coupling between localized and conduction electrons decreases as the Al content in the alloy increases.

I. INTRODUCTION

The Fe-rich Fe-Al alloys show very interesting magnetic properties.[1–4] At low Al concentration, up to 18 at. %, the alloys are ferromagnetic, independent of the heat treatment. From 18 to 33 at. % an ordered phase is formed, nonstoichiometric Fe_3Al. Finally, for larger Al content up to 51 at. % and by slow cooling from 700 °C, it forms the nonstoichiometric ordered FeAl phase. The experimental average magnetic moment extrapolated to 0 K, as shown by Vincze,[3] decreases with the Al concentration following a simple dilution model for Al content up to 25 at. %. In the range 25—30 at. % it shows a sudden fall followed by a slow variation until it becomes zero at 40 at. %. Several models have been proposed[2–7] to explain this strange behavior of the magnetic moment. More recently[8,9] careful measurements of the internal hyperfine magnetic field (HF) have been done on samples in the disordered phase by using the Mössbauer effect and a site diluted Ising model was proposed to explain the behavior of the average HF with temperature. The individual values of HF[8] can also give information about the local environment around a given Fe site. The possibility of theoretical interpretation of such data stimulates a microscopic description of the alloy.

In the present work we undertake an investigation of the electronic structure of disordered Fe-rich Fe-Al alloys by means of molecular cluster calculations. We focus our attention at electronic and magnetic properties at Fe sites in several possible local environments. The theoretical approach utilized in our study is briefly described in Sec. II. General features of the electronic structure of the alloy (density of states, charge transfer) are presented in Sec. III A. Our results for the hyperfine magnetic field at several Fe sites in the alloy are presented in Sec. III B. A discussion on local magnetic moments in the alloy is presented in Sec. III C. A brief summary of our results is presented in Sec. IV.

II. THEORETICAL APPROACH

A. Electronic structure

We use a localized description of the alloy by means of an "embedded-cluster" model.[10] This model has been already applied successfully to the study of electronic and magnetic properties of metal compounds and alloys.[10–12]

The clusters chosen to represent the alloy consist of a central Fe atom surrounded by 14 Fe or Al atoms [eight nearest neighbors (NN) and six next-nearest neighbors (NNN)] in an octahedral configuration compatible with the undistorted α-Fe lattice geometry (see Fig. 1). Some calculations have also been performed at three distinct

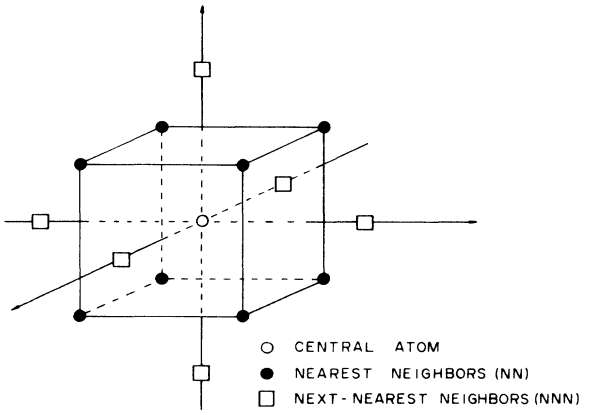

FIG. 1. 15-atom cluster representing a local environment in a bcc Fe-Al alloy.

values for the lattice parameter in order to study the effect of lattice expansion on the properties of the alloy. We have considered seven possible local environments around an Fe atom in the alloy, as follows: 8Fe NN + 6Fe NNN in O_h symmetry, (7Fe + 1Al) NN + 6Fe NNN in C_{3v} symmetry, (6Fe + 2Al) NN + 6Fe NNN in D_{3d} symmetry, (4Fe + 4Al) NN + 6Fe NNN in T_d symmetry, (4Fe + 4Al) NN + 6Fe NNN in C_{4v} symmetry, 8Fe NN + 6Al NNN in O_h symmetry, and 8Al NN + 6Fe NNN in O_h symmetry.

The electronic structure of the clusters was obtained by means of the first-principles self-consistent-charge discrete-variational method (SCC-DVM)[13–15] in the framework of local-density theory. The $X\alpha$ approximation[16] for the exchange potential,

$$V_{X\alpha}(\rho_\sigma) = -3\alpha \left[\frac{3\rho_\sigma(\mathbf{r})}{4\pi} \right]^{1/3} , \tag{1}$$

is used, with $\alpha = \frac{2}{3}$. The numerical basis set for the expansion of the wave function included $1s$, $2s$, $2p$, $3s$, $3p$, $3d$, $4s$, and $4p$ atomic orbitals for Fe and $1s$, $2s$, $2p$, $3s$, and $3p$ orbitals for Al. The atomic basis set was generated with potential wells around the atoms in order to obtain more contracted atomic valence orbitals. All electrons were given variational freedom in the cluster calculations which were carried to self-consistency.

An external pseudopotential is added to the molecular cluster potential to simulate the metal environment outside the cluster. Such an embedding scheme has been described elsewhere,[10] and consists of a superposition of atomic (Fe) potentials around the cluster. The external potential is truncated to simulate core orthogonality.

B. Isomer shifts and hyperfine magnetic fields

The calculation of the isomer shifts (IS) and the contact hyperfine fields (HF) involves small differences between large numbers. Therefore, special care must be taken regarding the numerical procedures. The isomer shift δ_{IS} in Mössbauer spectra can be related to the difference of densities $\rho(0)$ at the nuclei in source S and absorber A through

$$\delta_{IS} = \alpha[\rho_A(0) - \rho_S(0)] , \tag{2}$$

where α is a calibration constant which includes terms due to nuclear radii changes and relativistic effects.[11] Our calculations for δ_{IS} did not include the contributions from the deep-core $1s$ and $2s$ orbitals of Fe due to a limited numerical accuracy. Fortunately, atomic calculations for Fe in different oxidation states shows that those deep-core orbitals give negligible contributions to the difference density at the origin.[17]

The Fermi contact contribution to the hyperfine magnetic field is given by[18]

$$H_c = \tfrac{8}{3}\pi g \mu_B \frac{\langle S \rangle}{\mathscr{S}} [\rho_\uparrow(0) - \rho_\downarrow(0)] , \tag{3}$$

where S is the total spin of the ion with $\mathscr{S}$ unpaired electrons, g is the electronic g factor, μ_B is the Bohr magneton, and $\rho_\uparrow(0) - \rho_\downarrow(0) = \Delta\rho(0)$ is the spin density at the nucleus. The $3s$ and valence-band contributions to H_c are obtained in our calculations directly from the SCF molecular orbitals. The calculation of the deep-core $1s$ and $2s$ contributions requires, however, a different approach due to both numerical accuracy and basis-set uncompleteness; we perform atomic $X\alpha$ calculations for Fe in the configuration that corresponds to the Mulliken populations of the central Fe atom of the cluster. The $1s$ and $2s$ spin densities at the nucleus obtained from such atomic calculation are utilized to compute the corresponding contributions to H_c. We shall mention that a comparison with calculations for the FeO_4^{2-} ion[27] indicates that such approach may cause underestimations of about 6% on the H_c value.

III. RESULTS AND DISCUSSION

A. General features

Figures 2(a)–2(c) depict the partial density of states (PDOS) at the central Fe atom in three distinct cluster environments representing the Fe-Al alloy. The PDOS is defined as

$$\mathscr{D}(E) = B \left[\sum_i Q_i \delta(E - \epsilon_i) \right] , \tag{4}$$

where Q_i is the Mulliken population (at the central atom) of the ith molecular orbital of the cluster and B is a Lorentzian broadening function, to simulate a continuum. Figure 2(a) shows the PDOS of the "perfect" iron cluster, which shows quite good agreement with the density of states obtained in band-structure calculations.[20] In Fig. 2(b) we show the PDOS for the (4Fe + 4Al) NN + 6Fe NNN T_d environment (four aluminum nearest neighbors in T_d symmetry) and in Fig. 2(c) we show the PDOS for the 8Al NN + 6Fe NNN environment, both at the undistorted iron geometry with a lattice constant of 2.866 Å.

Some general features can be observed in the PDOS's of Fig. 2, as we go into the direction of increasing number of Al nearest neighbors:

(i) The energy splitting between the main (majority and minority spin) $3d$ peaks is not modified, but the Fermi level moves toward the minority spin $3d$ main peak; as a result, the $3d$ local magnetic moment decreases with increasing number of aluminum neighbors.

(ii) The two greater $3d$ peaks of minority spin tend to collapse into a single broad peak. All the rest of the secondary-peak structures below E_F (including the $4s + 4p$ structure) tend to broaden and disappear; this can be seen as a "fingerprint" of the loss of magnetic coupling between the central iron atom and its environment, as the number of iron nearest neighbors is reduced.

Charge transfer seems to play a minor role in the properties of the disordered Fe-Al alloys; no isomer shift (IS) was detected within the experimental accuracy.[21] This is consistent with our calculated results for IS in clusters with up to four Al neighbors (at a lattice parameter of 2.866 Å), which show shifts smaller than 0.05 mm/s (see Fig. 3). The charge transfer (in the Mulliken approach) for the clusters cited above is also small, being less than 0.09 electrons in all cases. The IS of the 8Al NN cluster (0.09 mm/s at the perfect α-Fe lattice parameter) could be measured in principle, but such a configuration is very unlikely to occur in a disordered Fe-Al alloy. The IS also

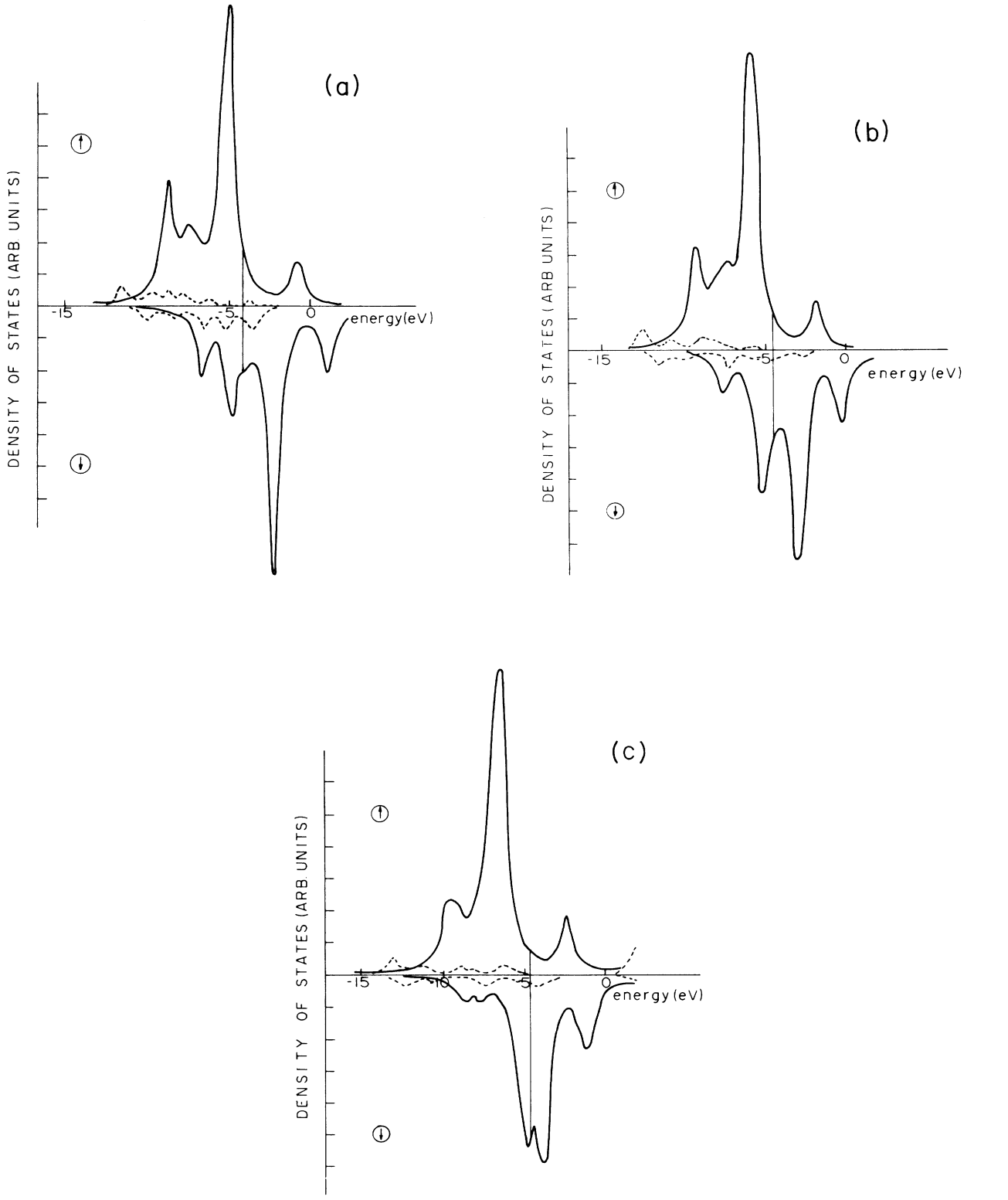

FIG. 2. Partial density of states (PDOS) at the central iron atom in three distinct environments representing a disordered Fe-Al alloy; (a) the "perfect" α-Fe environment, with 8Fe nearest neighbors (NN) and 6Fe next-nearest neighbors (NNN); (b) the environment with (4Fe + 4Al) NN + 6Fe NNN in T_d symmetry; (c) the environment with 8Al NN + 6Fe NNN. The spin ↑ and spin ↓ bands are normalized to the same scale (within each environment). The vertical bar indicates the Fermi level. The solid curves correspond to the $3d$ contributions to the PDOS, and the dashed ones to the $4s + 4p$ contributions.

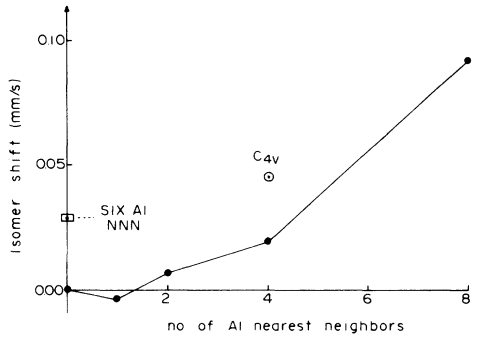

FIG. 3. Calculated isomer shifts (IS) at the central iron atom in several distinct environments representing a disordered Fe-Al alloy. The dots (●) connected by solid lines indicate the calculated values for environments with 6Fe next-nearest neighbors (NNN) and a variable number of aluminum nearest neighbors (NN) in the highest possible symmetry. The separate point (⊙) indicates the IS for the environment with 4Al NN (otherwise Fe) in C_{4v} symmetry. The point (⊡) indicates the value for the environment with 6Al NNN (otherwise Fe). A nuclear parameter (calibration constant) $\alpha=-0.25$ mm a_0^3/s is used (Ref. 11) in all calculations.

shows a linear variation with lattice parameter in the range we have considered (5.4—5.6 a.u.); three distinct clusters [(4Al + 4Fe) NN + 6Fe NNN, 8Al NN + 6Fe NNN, and 8Fe NN + 6Al NNN] showed about the same variation $\Delta(\text{IS})=0.10$ mm/s for a 1% volume change, which is also close to the value for bcc iron under pressure.[22] The symmetry of the local environment around an Fe atom seems to strongly affect the charge transfer and the isomer shift. For instance, the cluster with 4Al nearest neighbors in C_{4v} symmetry gives values of isomer shift (see Fig. 3) and charge transfer about twice as large as the values for the T_d symmetry environment. The presence of aluminum next-nearest neighbors (NNN) also affects the IS and the charge transfer at the central atom. The cluster with 6Al NNN shows IS and charge transfer about 30% as large as that of the cluster with 8Al NN. In that sense, we might say that a 15-atom cluster model may be not large enough to describe quantitatively the alloy environment effects on IS and charge transfer.

B. Hyperfine magnetic fields

We have performed calculations for the contact spin density $\Delta\rho(0)$ at the nucleus of the central Fe site in the perfect iron environment. We obtained the values (in a.u.$^{-3}$) -0.048, -1.266, 0.518, and -0.007 for $\Delta\rho_{1s}(0)$, $\Delta\rho_{2s}(0)$, $\Delta\rho_{3s}(0)$, and $\Delta\rho_{4s+4p}(0)$, respectively, where $\Delta\rho_n(0)$ is the contact spin density for the nth set of molecular-orbital levels of a particular atomic character. The hyperfine magnetic field can be calculated in the "contact" approximation (see Sec. II B) through

$$H_{\text{hf}}\cong H_c=524.2\Delta\rho(0)\ \ (\text{in kG})\ . \tag{5}$$

We obtain $H_c=-421$ kG, which is about 30% too large as compared to the experimental value,[23] -339 kG. We should point out that, apart from cluster-size effects, both the form of the local exchange used[24] and relativistic effects[25] can strongly affect the H_{hf} result in a local-density calculation.

We have also calculated the contact hyperfine field H_c for six distinct local configurations representing the alloy. In Fig. 4 and Table I we show our results (for a lattice parameter of 2.866 Å) in the form

$$\Delta H_{\text{hf}}=H_c(\text{alloy})-H_c(\text{iron})\ , \tag{6}$$

where H_c(iron) is the calculated H_c for the perfect iron cluster and H_c(alloy) is calculated for a cluster representing a given local configuration in the alloy. We predict changes of about + 25 kG for each Fe atom replaced by an Al atom in the first shell of neighbors, and changes of about + 2.6 kG for similar replacements in the second shell of neighbors. The contribution of the valence electrons to ΔH_{hf} is dominant, and accounts for $\sim 80\%$ of the total value.

Our results for ΔH_{hf} (specially for the first shell of neighbors) are in good agreement with experimental results[2,8,24] obtained from Mössbauer effect measurements which are also depicted in Fig. 4 and Table I. We shall mention that the effects above mentioned which can affect the calculation of H_c (iron) are partially cancelled with H_c (alloy) when we calculate ΔH_{hf}. This may be partially responsible for the observed good agreement between our results and experiment. It is also worth mentioning that the experimental results shown in Table I were obtained at room temperature; comparison with measurements performed at liquid nitrogen[8] indicates that, although the absolute $|H_{\text{hf}}|$ values shall increase by about 7 kG on extrapolating to close-to-zero Kelvin temperatures, the ΔH_{hf} values shall decrease by less than 2

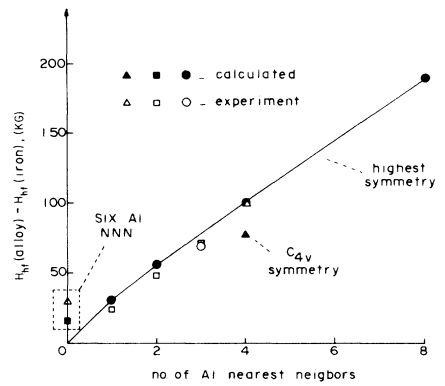

FIG. 4. Deviation (ΔH_{hf}) from the hyperfine field of the perfect α-iron at the central iron atom in several distinct environments representing a disordered Fe-Al alloy. The dots (●) connected by solid lines indicate the calculated values for environments with 6Fe next-nearest-neighbors (NNN) and a variable number of aluminum nearest neighbors (NN) in the highest possible symmetry. The point (▲) indicates ΔH_{hf} for the environment with 4Al NN (otherwise iron) in C_{4v} symmetry. The point (■) indicates ΔH_{hf} for the environment with 6Al NNN (otherwise Fe). The points (□, ○, △) indicate some experimental results; (□), Ref. 8; (○), Ref. 2; (△), Ref. 26.

TABLE I. Hyperfine magnetic fields (H_{hf}) for different iron sites in Fe-rich Fe-Al alloys. ΔH_{hf} is the difference between the H_{hf} at a given site and the H_{hf} at the site with eight Fe nearest neighbors and six Fe next-nearest neighbors (8Fe NN + 6Fe NNN). The experimental results were obtained at room temperature; the calculated results corresponds to SCF molecular cluster calculations at the pure α-iron lattice parameter.

Environment	$\lvert H_{hf} \rvert$, expt. (kG)	ΔH_{hf}, expt. (kG)	ΔH_{hf}, calc. (kG)
8Fe NN + 6Fe NNN	330[a]	0	0
(7Fe + 1Al) NN + 6Fe NNN	306[a]	24	31
(6Fe + 2Al) NN + 6Fe NNN	282[a]	48	56
(5Fe + 3Al) NN + 6Fe NNN	261[b]; 258[a]	69; 72	
(4Fe + 4Al) NN + 6Fe NNN	230[c]	100	102
(4Fe + 4Al) NN + 6Fe NNN(C_{4v})			77
8Al NN + 6Fe NNN	0[d]	330	191
8Fe NN + 6Al NNN	300[c]	30	16

[a]Reference 8.
[b]Reference 2.
[c]Reference 26.
[d]Obtained for the nonmagnetic FeAl ordered phase, see Ref. 8.

kG (at $\gtrsim 0$ K) due to cancellations. Figure 4 also shows that ΔH_{hf} is at least five times more affected by the presence of an aluminum nearest neighbor than by the presence of an aluminum next-nearest neighbor. In that sense, we can say that ΔH_{hf} is a short-range parameter.

We have also studied the effects of lattice parameter variation and the variation of the symmetry of the local environment on the hyperfine fields. The latter parameter variation little affects the H_{hf} values; a variation of 0.5% of the lattice constant above the perfect iron spacing (which corresponds to an Al content in the alloy of about 10%, a typical concentration for H_{hf} measurements[8]) causes an increase of H_{hf} by 3.3 kG for the environment 8Al NN + 6Fe NNN, 1.8 kG for the environment (4Fe + 4Al) NN + 6Fe NNN, and 1.4 kG for the environment 8Fe NN + 6Al NNN. The corresponding change on α-Fe under pressure[22] (obtained through Mössbauer measurements) is 1.85 kG. The symmetry of the local environment seems to play a significant role on the hyperfine fields; for instance, the H_{hf} for the (4Fe + 4Al) NN + 6Fe NNN environment in (less probable[27]) C_{4v} symmetry is about 8% smaller than that of the corresponding T_d symmetry environment (see Fig. 4), and would be undistinguishable from the H_{hf} of the 3Al NN environment in a Mössbauer measurement.[8]

C. Magnetic moments

Figure 5 shows the behavior of the magnetic moment μ_{Fe} on the central iron atom as a function of the number of aluminum neighbors for a lattice parameter of 2.866 Å. The total μ_{Fe} shows a small increase with the addition of Al atoms in the first shell of neighbors. The partial $3d$ component μ_{3d} of the moment shows a small decrease caused by the shift of the Fermi level, as already discussed in Sec. III A.

An interesting feature also depicted in Fig. 5 is the behavior of the partial $4s + 4p$ (conduction band) μ_{band} component of the magnetic moment. Its negative value for the perfect iron cluster ($\mu_{band} = -0.34\ \mu_B$) can be ascribed to the effective antiferromagnetic exchange J_{eff} between localized and conduction electrons in ferromagnetic materials.[28] The addition of Al atoms from zero up to about six aluminum nearest neighbors results in a decreases of $\lvert \mu_{band} \rvert$. A further addition of Al nearest neighbors results in a positive value for μ_{band}. This result

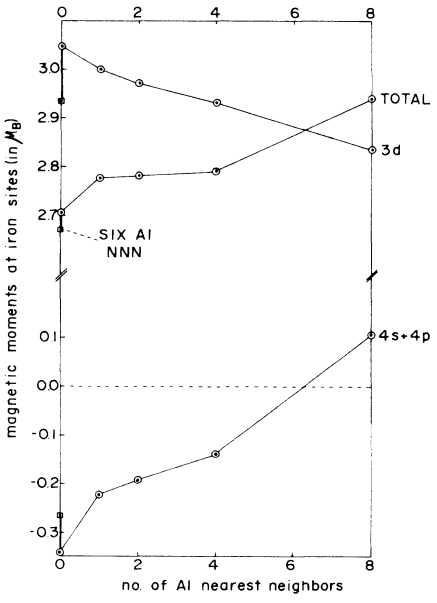

FIG. 5. Calculated values for the magnetic moment (μ_{Fe}) of the central Fe atom in several distinct environments representing a disordered Fe-Al alloy. The points (⊙) connected by solid lines indicate the values for environments with 6Fe next-nearest neighbors (NNN) and a variable number of Al nearest neighbors (NN) in the highest possible symmetry. The points (⊡) indicate the values for the environment with 6Al NNN (otherwise Fe). The partial contributions $3d$ and $4s + 4p$ to the moment are also depicted.

indicates that $|J_{\text{eff}}|$ should decrease with the increase of Al content in the alloy, with a subsequent reduction of the magnetic ordering temperature. This fact is observed experimentally.[8] The results for the 8Fe NN + 6Al NNN configuration are also shown in Fig. 5. The value of μ_{band} is more affected by the presence of *one* Al nearest neighbor than by the presence of *six* Al next-nearest neighbors. This result could explain the success of the nearest-neighbor interaction Ising model on the description of thermodynamical properties of Fe-Al alloys.[8,9]

The behavior of the magnetic moment μ_{Fe} ($3d + 4s + 4p$ on the central Fe atom) with the variation of lattice parameter is shown in Fig. 6 for three distinct environments, i.e., (4Al + 4Fe) NN + 6Fe NNN, 8Al NN + 6Fe NNN, and 8Fe NN + 6Al NNN. The three configurations show maxima for μ_{Fe} in the range of lattice distances we have considered. One can see that the derivative $d(\mu_{\text{Fe}})/da$ at the lattice parameter of pure α-Fe (2.866 Å) increases as we put more aluminum atoms in the first shell of neighbors. The partial $3d$ component μ_{3d} of the moment is an increasing monotonic function of the lattice parameter; the maxima observed in μ_{Fe} are due to the decrease of the $4s + 4p$ component μ_{band}.

We have also performed calculations on a cluster with a central aluminum atom in a perfect iron environment ($AlFe_8Fe_6$); we obtain a local moment on the central Al atom (μ_{Al}) of $-0.7\mu_B$. This corresponds to a *decrease* of $0.4\mu_B$ in the conduction-band magnetic polarization at the central atom if we replace Fe by Al. Therefore, we have two competitive effects on the conduction-band polarization; an increase of μ_{band} on the Fe atoms close to Al sites (see Fig. 5), and a decrease of the conduction-band moment at Al sites. The 15-atom cluster model utilized in the present work predicts that the increase of $\mu(\text{Fe})_{\text{band}}$ is the dominant effect; however, larger cluster calculations would be required to study the balance between the two effects in a more reliable way.

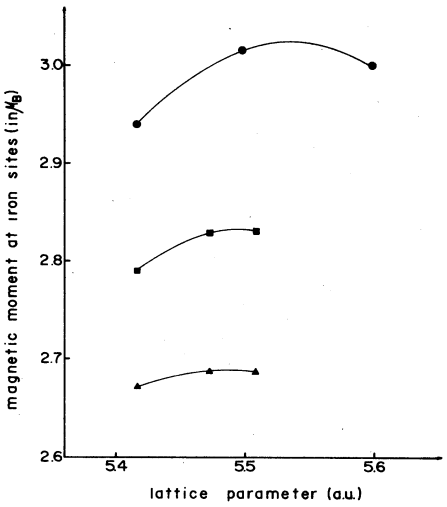

FIG. 6. Lattice parameter dependence of the magnetic moment (μ_{Fe}) at the central Fe atom in three distinct environments representing a disordered Fe-Al alloy. The points (●) indicate SCF calculations for the environment with 8Al nearest neighbors (NN) and 6Fe next-nearest neighbors (NNN), the points (■) indicate SCF calculations for the (4Fe + 4Al) NN + 6Fe NNN environment and the points (▲) indicate SCF calculations for the 8Fe NN + 6Al NNN environment. The points are connected by fitted parabolas.

IV. SUMMARY

We have performed first-principles self-consistent-field calculations for the electronic structure of clusters representing disordered Fe-rich Fe-Al alloys. Several possible environments of atoms around iron sites in the alloy have been considered in order to study properties such as the density of states, charge transfer and isomer shifts, magnetic moments and hyperfine fields. The effect of the lattice parameter variation on the above mentioned quantities was also investigated.

The partial density of states at a given Fe site in the alloy shows loss of structure as we replace Fe neighbors by aluminum. We interpret this fact as the loss of magnetic coupling between the Fe atom and its environment. Charge transfer seems not to be important to the properties of the alloy; we estimate that isomer shifts (IS) shall be smaller than 0.05 mm/s for the range of Fe concentration in which the disordered phase occurs. The IS is determined not only by the number of Al nearest neighbors; the effect of lattice expansion, the symmetry of the local environment and the presence of Al next-nearest neighbors are also found to affect the shift.

Our results for the variations of the hyperfine magnetic field (HF) at iron sites due to the presence of aluminum neighbors are in very good agreement with experiments. The HF is mainly determined by the number of Al nearest neighbors, but it is also affected by the presence of Al next-nearest neighbors, by lattice expansion and by the symmetry of the local environment.

Our calculations show that the $3d$ component of the magnetic moment at Fe sites decreases as the number of Al neighbors increases, as a result of the variation of the Fermi level. The corresponding conduction-band component (at Fe sites) becomes less negative, which indicates that the antiferromagnetic exchange between conduction and localized electron decreases as the Al content in the alloy increases.

ACKNOWLEDGMENTS

This research was supported by the Brazilian agencies Financiadora de Estudos e Projetos and Conselho Nacional de Desenvolvimento Cientifico e Tecnológico and by the National Science Foundation (NSF) grant No. 10110038/82. DEE was supported by the Fullbright Foundation and thanks the Fullbright Commission in Brazil for their help.

[1]A. Arrott and H. Sato, Phys. Rev. **114**, 1420 (1959).
[2]G. P. Huffman and R. M. Fisher, J. Appl. Phys. **38**, 735 (1967).
[3]I. Vincze, Phys. Status Solidi (A) **7**, K43 (1971).
[4]M. Shiga and Y. Nakamura, J. Phys. Soc. Jpn. **40**, 1295 (1976).
[5]H. Sato and A. Arrott, Phys. Rev. **114**, 1427 (1959).
[6]P. Shukla and M. Wortis, Phys. Rev. B **21**, 159 (1980).
[7]G. S. Grest, Phys. Rev. B **21**, 165 (1980).
[8]G. A. Perez Alcazar and E. Galvão da Silva (unpublished).
[9]G. A. Perez Alcazar, J. A. Plascak, and E. Galvão da Silva, Phys. Rev. B **34**, 1940 (1986).
[10]D. E. Ellis, G. A. Benesh, and E. Byrom, Phys. Rev. B **20**, 1198 (1979).
[11]D. Guenzburger and D. E. Ellis, Phys. Rev. B **31**, 93 (1985).
[12]D. E. Ellis and D. Guenzburger, Phys. Rev. B **31**, 1514 (1985).
[13]E. S. Baerends, D. E. Ellis, and P. Ros, Chem. Phys. **2**, 41 (1973).
[14]A. Rosen, D. E. Ellis, H. Adachi, and F. W. Averill, J. Chem. Phys. **65**, 3629 (1976).
[15]B. Delley and D. E. Ellis, J. Chem. Phys. **76**, 1949 (1982).
[16]J. C. Slater, *The Self-Consistent Field for Molecules and Solids* (McGraw-Hill, New York, 1974).
[17]N. N. Greenwood and T. C. Gibb, *Mössbauer Spectroscopy* (Chapman and Hall, London, 1971).
[18]R. E. Watson and A. J. Freeman, Phys. Rev. **123**, 2027 (1961).
[19]D. Guenzburger, D. M. S. Esquivel, and J. Danon, Phys. Rev. B **18**, 4561 (1978).
[20]V. L. Moruzzi, J. F. Janak, and A. R. Williams, *Calculated Electronic Properties of Metals* (Pergamon, New York, 1978).
[21]E. Galvão da Silva and G. A. Perez Alcazar (unpublished).
[22]D. L. Williamson, S. Bukshpan, and R. Ingalls, Phys. Rev. B **6**, 4194 (1972).
[23]C. E. Violet and D. N. Pipkorn, J. Appl. Phys. **42**, 4339 (1971).
[24]J. Calleway and C. S. Wang, Phys. Rev. B **16**, 2095 (1977).
[25]J. J. Mallow, A. J. Freeman, and J. P. Desclaux, Phys. Rev. B **13**, 1884 (1976).
[26]K. Ono, Y. Ishikawa, and A. Ito, J. Phys. Soc. Jpn. **17**, 1747 (1962).
[27]G. Inden and W. Pitsch, Z. Metallkd. **62**, 627 (1971); **63**, 253 (1972).
[28]A. Blandin, in *Magnetism* Vol. V of *Magnetic Properties of Metallic Alloys* (Academic, New York, 1973).